Talanta 84 (2011) 853–858

Contents lists available at ScienceDirect

Talanta

journal homepage: www.elsevier.com/locate/talanta

Study of mineralogical speciation of arsenic in soils using X ray microfluorescence and scanning electronic microscopy

Isidoro Gómez-Parrales, Nicolás Bellinfante, Manuel Tejada*

Departamento de Cristalografía, Mineralogía y Química Agrícola. Universidad de Sevilla. Ctra. de Utrera, km. 1. 4013, Sevilla, Spain

ARTICLE INFO

Article history:
Received 21 October 2010
Received in revised form 31 January 2011
Accepted 14 February 2011
Available online 19 February 2011

Keywords:
Arsenic in soils
X-ray microfluorescence
SEM–BEI–EDX
Mineralogical speciation

ABSTRACT

In this paper we studied the As content in natural contaminated soils, classified as Dystric Leptosol, Chromic Luvisol, Eutric Cambisol and Mollic Leptosol. In soil samples, sieved (<2 mm), total As was determined by XRF and chemical speciation by sequential extraction. As-bearing minerals were concentrated from fine sand fraction of soil (200–20 μm) using heavy liquid. In this fraction, mineralogical speciation was studied by X-ray microfluorescence, XRD with Göbbel mirror and SEM–BEI–EDX. Total As contents ranging from 61.00 to 131.00 mg kg^{-1}. The results of the sequential extraction showed that As was, mainly, in the residual fraction (52.51–98.76 mg kg^{-1}) and in the fraction bound to iron oxyhydroxides (0–36.5 mg kg^{-1}). Mapping of As with X-ray microfluorescence show strongly relationship between Fe and As. Iron (III) oxyhydroxides (FeOHs) (lepidocrocite and goethite), scorodite, angelellite, schultenite and dussertite were identified by XRD analysis as most likely mineral phases. The contents of As, Fe, Pb and Ba obtained with EDX-microprobe, confirmed the results of XRD. The results of sequential extraction and X-ray microfluorescence indicate that As is strongly bound to the soils because the identified As-bearing mineral phases are very stable at the pH conditions of studied soils. Consequently, a low mobility of As can be assumed in these soils.

1. Introduction

Arsenic is a trace element of great interest for scientists who study the environment due to its high risk to human health [1,2]. Arsenic can be released into the environment either by natural processes (volcanism or alteration of the rock) or by anthropogenic sources (e.g. mining, metal ores processing, agricultural, pesticide manufacture, etc.) [3–6].

There are several works devoted to understand the behavior of arsenic in soils [6–10]. However, few authors treat arsenic pollution from natural sources [11–14]. In environmental law this is of great importance to establish the threshold value from which a soil is considered contaminated.

Generally, the arsenic soil content depend on various parameters such as mineralogical and chemical composition of parent material, soil forming processes, texture, mineralogy of clay fraction, organic matter content, carbonate, iron oxyhydroxides content, aluminum and manganese, etc. [15–18]. Therefore, the arsenic content varies significantly from one location to another. In recent years, the chemical fraction of arsenic in soil has become very important, since its toxicity depends on the chemical and mineralogical forms.

In recent literature there are different analytical techniques that allow to determine the chemical fractionation [19–21] and mineralogy of arsenic [6,22,23]. These techniques are helpful in determining the easily mobilizable arsenic and the risk of arsenic contamination in soils. The chemical fractionation raises some problems related to the specificity of the reagents used and the arsenic solubilization. On the other hand, mineralogical speciation, mainly determined by XRD and scanning electronic microscopy (SEM) with microprobe [10,22,24], provides direct information on the amount of adsorbed arsenic, as well as mineral phases found in the metal. Therefore, analytical techniques to determine the mineralogical species can help to asses labile fractions of trace elements like arsenic and consequently the degree of mobility.

The two main objectives of this study were: (1) propose a methodology based on the use of instrumental techniques for studies on mineral speciation of arsenic in soil and thus help to determine the labile fraction of this element, and (2) to compare the data obtained in the sequential extraction with the results of mineralogical studies.

2. Material and methods

2.1. Site description and soil sampling

The study area is located in the "Valle de los Pedroches" (northern province of Córdoba, Spain). This area consists of a

* Corresponding author. Tel.: +34 9544 864 64; fax: +34 9544 864 36.
E-mail address: mtmoral@us.es (M. Tejada).

0039-9140/$ – see front matter © 2011 Elsevier B.V. All rights reserved.
doi:10.1016/j.talanta.2011.02.010

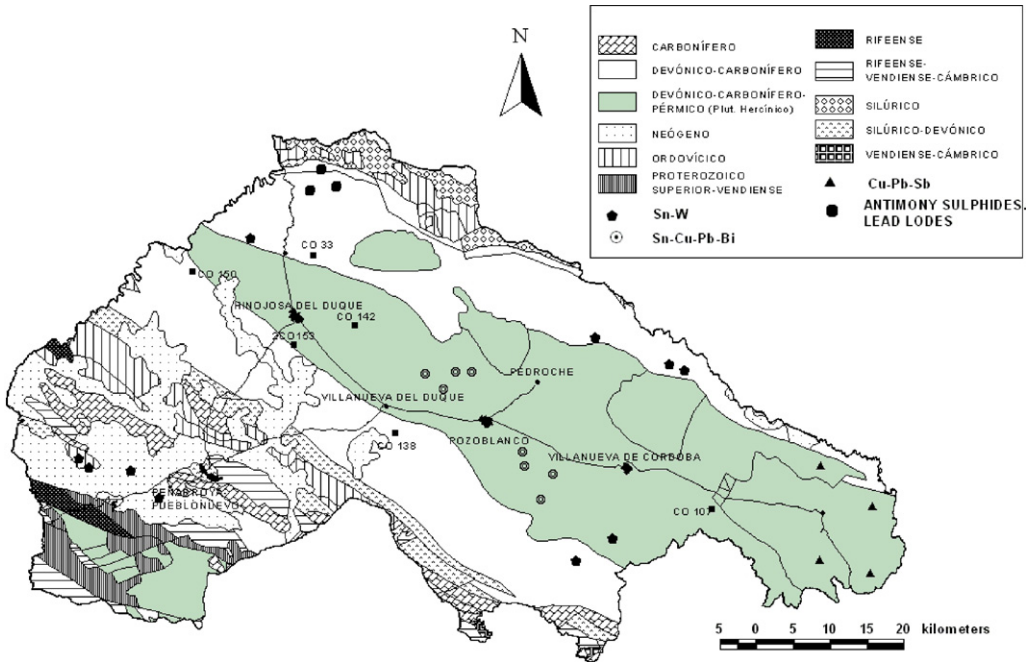

Fig. 1. Localization of samples. Geologic and metalisations map of study area.

Table 1
Soil samples identification.

Soil classification	Soil profile	Depth	Soil identification
Dystric Leptosol	Co-33	1	Co-33-1
Chromic Luvisol	Co-150	1	Co-150-1
		2	Co-150-2
Eutric Cambisol	Co-138Co	1	Co-138-1
		2	Co-138-2
	Co-142	1	Co-142-1
		2	Co-142-2
	Co-153	1	Co-153-1
		2	Co-153-2
Mollic Leptosol	Co-107	1	Co-107-1

Depth: 1 (0–20 cm); 2 (20–40 cm).

granitic batholith with NW–SE direction. This batholith is composed of granites, granodiorites and diorites with porphyrites, microgranitic, microdioritas and aplite [25].

Fig. 1 shows the geologic and mineralisation maps of the study area, as well as, the localization of samples. In the easterly region of the batholith, a zoned Cu–Pb–Sb mineralisation is developed. The copper lodes are chiefly chalcocite–chalcopyrite–quartzcarbonate bearing and are located preferentially in the biotite granite. The argentiferous lead lodes contain a gangue of mainly quartz and local barites and are situated chiefly in the northern margin of the granite and country rocks. Antimony sulphides and oxides in quartz veins outcrop in the country rocks north of the batholith. Sn–W lodes in association with As, Cu, U, Ag, Bi, Ni, Co, and Pb mineralisation are located mainly near the margins of the batholith. In the central regions of the batholith there is considerable tin, copper, lead and bismuth mineralisation. The bismuth mineralisation is of economic or sub economic importance and is located with Ni–Co–As–Ag–Au assemblages in dominantly NNE–SSW trending fissure veins cutting contact hornfelses.

Sampling sites were conducted in soils with high content in As The samples were taken at two depths (0–20 and 20–40 cm). For Leptosols we only sampled the topsoils (0–20 cm). In total, 10 samples were selected corresponding to 6 soil profiles, classified as: Dystric Leptosol (Co-33), Chromic Luvisol (Co-150), Eutric Cambisol (Co-138, Co-142 and Co-153) and Mollic Leptosol (Co-107) (Table 1) (FAO-ISRIC-ISSS [26]).

After air drying, soil samples were ground to pass a 2-mm sieve and stored in sealed polyethylene bags until analysis.

2.2. Soil analytical determinations

2.2.1. Determination of pH

pH was determined with distilled water in 1:2.5 soil:water ratio [27]

Table 2
Total content, bioavailability and sequential extraction [19] of arsenic in soils (mg kg^{-1}).

Sample	Total	Acid water (pH 1)	EDTA	Exchangeable	Carbonates	Fe and Mn oxides	Organic matter	Residual fraction
Co-33-1	80.00	<0.03	<0.03	<0.03	<0.03	27.49	<0.03	50.51
Co-107-1	131.00	<0.03	<0.03	<0.03	<0.03	32.04	<0.03	101.16
Co-138-1	76.00	<0.03	<0.03	<0.03	<0.03	<0.03	<0.03	77.90
Co-138-2	63.00	<0.03	<0.03	<0.03	<0.03	<0.03	<0.03	62,17
Co-142-1	109.00	<0.03	<0.03	<0.03	<0.03	36.42	<0.03	70.58
Co-142-2	99.00	<0.03	<0.03	<0.03	<0.03	36.35	<0.03	63.65
Co-150-1	91.00	<0.03	<0.03	<0.03	<0.03	<0.03	<0.03	91.64
Co-150-2	88.00	<0.03	<0.03	<0.03	<0.03	<0.03	<0.03	87.20
Co-153-1	61.00	<0.03	<0.03	<0.03	<0.03	<0.03	<0.03	61.39
Co-153-2	61.00	<0.03	<0.03	<0.03	<0.03	<0.03	<0.03	61.54

Table 3
Content in amorphous and total iron of soil samples.

Element	Fe_o	Fe_t
Co-33-1	0.44	5.23
Co-107-1	0.35	5.98
Co-138-1	0.27	3.89
Co-138-2	0.24	4.13
Co-142-1	0.31	5.17
Co-142-2	0.28	5.63
Co-150-1	0.35	8.75
Co-150-2	0.30	9.86
Co-153-1	0.22	4.76
Co-153-2	0.24	5.31

Table 4
Chemical analysis (wt%) of samples with highest arsenic contents using EDX.

Element	Co-107	Co-142-1	Co-142-2	Co-150-1	Co-150-2
O	49.61	41.40	47.62	30.79	20.85
Mg	0.70	ND	ND	ND	ND
Al	6.30	3.49	5.74	2.86	1.99
Si	7.42	4.85	4.6	2.55	2.13
P	0.81	ND	2.52	0.47	0.93
S	ND	1.11	ND	ND	ND
K	0.30	0.52	0.18	0.16	0.15
Ca	0.56	1.28	0.28	0.89	0.81
Ti	0.70	1.14	0.2	0.41	0.4
Mn	0.12	ND	ND	0.42	0.58
Fe	32.62	25.94	26.33	39.12	47.6
Cu	0.21	0.68	0.26	0.46	0.44
Zn	ND	ND	0.36	ND	ND
As	0.65	4.50	3.17	18.9	21.33
Pb	ND	15.08	8.75	ND	ND
Ba	ND	ND	ND	2.97	2.79

ND: not detected.

Table 5
Arsenic contents in the fraction of 200–50 μm determined by X-ray microfloures-cence (spot diameter, 300 μm).

Sample	As (%)
Co-33-1	0.30
Co-107-1	0.75
Co-138-1	0.15
Co-138-2	0.25
Co-142-1	0.65
Co-142-2	0.59
Co-150-1	0.52
Co-150-2	0.53
Co-153-1	0.1
Co-153-2	0.09

2.2.2. Determination of amorphous iron

Amorphous iron was determined by Shwertman method [27]

2.2.3. Chemical fractionation

2.2.3.1. Total arsenic. Twelve grams of soil were ground in a planetary ball mill FRITSCH Pulverisette 6 with a bowl of milling (grinding bowl) and WC balls. Subsequently, the soil was sieved to 100 μm. The total arsenic content was determined by XRF spectrometer with X-ray fluorescence Panalytical AXIOS model.

2.2.3.2. Extraction with EDTA and acidic water. These fractions determine the arsenic mobility in soils [28,29].

To determine the fraction extractable with EDTA, 2.5 g of soil were shaken with 25 mL of 0.05 M EDTA (pH 7). For the acidic water-extractable fraction is produced in the same way but using 25 mL of water adjusted to pH 1 with HNO_3.

2.2.3.3. Sequential extraction. Sequential extraction was performed using the Tessier et al. [19] method. Several authors [30,31] have used the Tessier et al's method for metal studies in soils. This method separates the following fractions:

- Fraction 1. Exchangeable. 1 g air-dry soil was extracted at room temperature for 1 h with 8 mL of $MgCl_2$ 1 M.
- Fraction 2. Bound to carbonates. The residue from the fraction 1 was leached at room temperature for 5 h with 8 mL of 1 M NaOAc (pH 5).
- Fraction 3. Bound to Fe–Mn oxides. The residue from the fraction 2 was extracted for 6 h with 20 mL of 0.04 M NH_2OH HCl in 25% (v/v) HOAc.
- Fraction 4. Bound to organic matter. To the residue from the fraction 3 were added 3 mL of 0.02 M HNO_3 and 5 mL of 30% H_2O_2 (pH 2 with HNO_3) and the mixture was heated to 85 ± 2 °C for 2 h with occasional agitation. A second 3-mL aliquot of 30% H_2O_2 (pH 2 with HNO_3) was then added and the sample was heated again to 85 ± 2 °C for 2 h with intermittent agitation. After cooling, 5 mL of 3.2 M NH_40Ac in 20% (v/v) HNO_3 was added and the sample was diluted to 20 mL and agitated continuously for 30 min.
- Fraction 5. Residual. The residue from (iv) was digested with a HF-HC104 mixture according to the procedure described below for total metal analysis.

All extraction were conducted in a vibrator stirrer model "Selecta Rocking Mixer Vibromatic". The extracts were centrifuged at 10,000 rpm for 15 min. The supernatant was filtered with Whatmann no. 42 filter paper.

The arsenic content in each of the fractions was determined by ICP–AES using an atomic emission spectrometer ICP plasma Fisons-ARL 3410.

2.2.4. Mineralogical speciation

Mineralogical speciation was carried out with samples that showed a higher total arsenic.

Firstly, the fine sand fraction (200–20 μm) were separated by sieving. Subsequently, the heavy minerals were separated with bormoform ($d = 2.89\ g\ cm^{-3}$). In this fraction the following determinations were made:

2.2.4.1. Arsenic mapping. Iron and arsenic mapping was performed in the soil samples with highest arsenic contents using X-ray microfluorescence (EDAX Eagle III model). The objective of this mapping was to obtain the spatial distribution of both elements to establish possible associations between them.

2.2.4.2. X-ray diffraction analyses (XRD). A diffractometer Bruker D8 C equipped with Göbel mirror, with the following conditions was used: CuKα radiation, 40 kV, 40 mA, step size 0.03°/s in the range of 3–70° 2θ. For the identification of mineral phases XPowder ver. 2004.04.46 PRO and PDF-2 database were used.

2.2.4.3. Scanning electron microscopy and energy dispersive X-ray microanalysis. Images were obtained from selected soil samples

Table 6
Values of pH in water (1:2.5 soil:water ratio).

Sample	pH
Co-33-1	5.5
Co-107-1	4.8
Co-138-1	4.8
Co-138-2	4.6
Co-142-1	5.3
Co-142-2	5.0
Co-150-1	4.8
Co-150-2	4.6
Co-153-1	5.1
Co-153-2	5.4

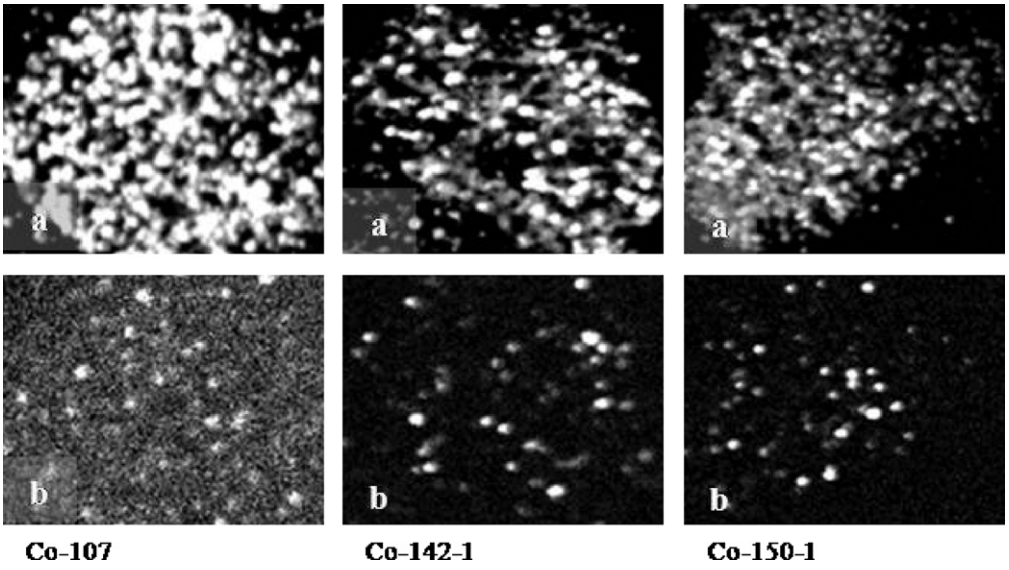

Fig. 2. Microfluorescence mapping. White points indicate spatial distribution of iron (a) and arsenic (b) content in samples.

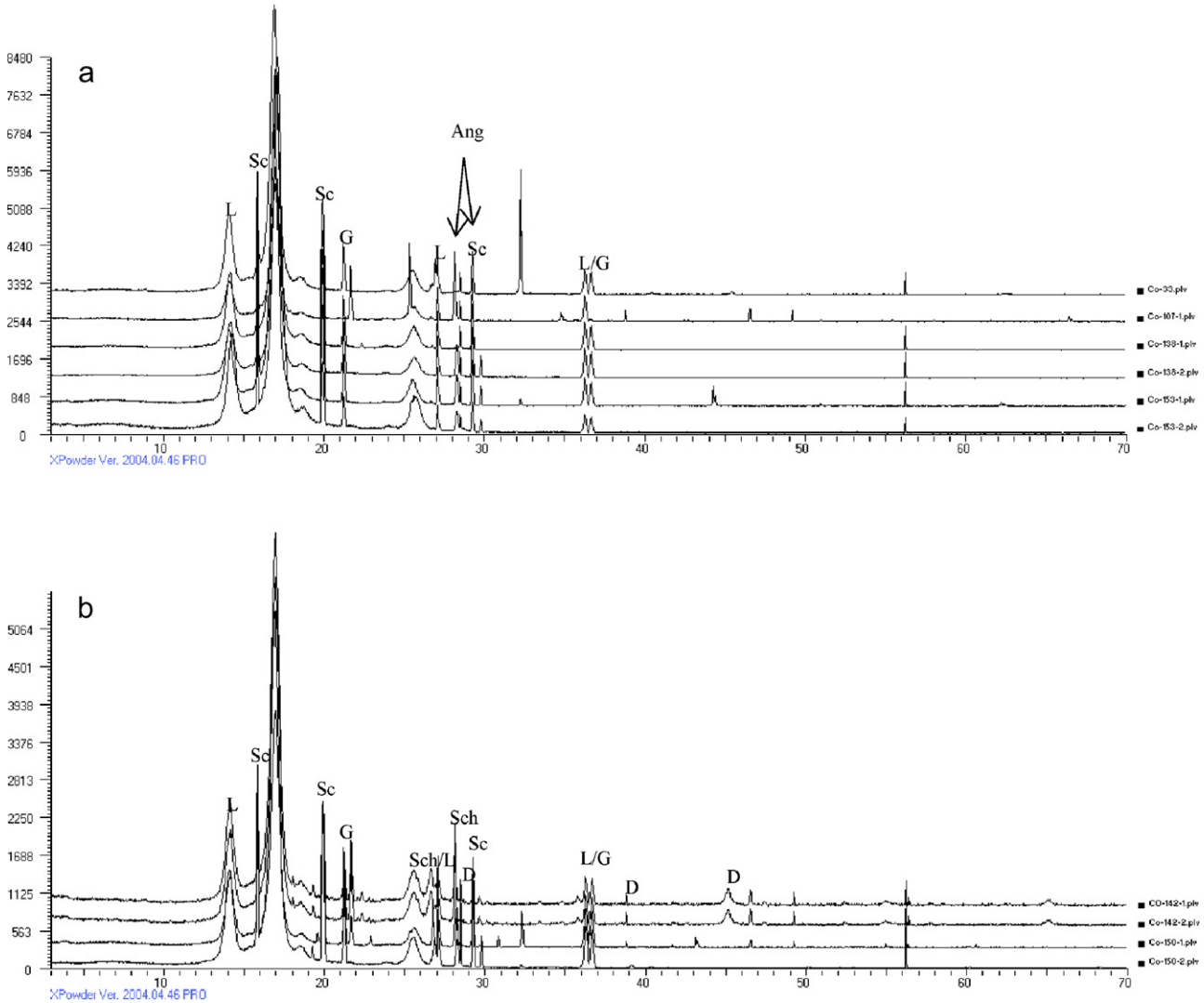

Fig. 3. XRD: (a) Co-33; Co-107-1; Co-138-1; Co-138-2; Co-153-1; Co-153-2; Co-138-1; Co-138-2; (b) Co-142-1; Co-142-2; C0-150-1; Co-150-2. Ang: Angelellite; G: Goethite; L: Lepidocrocite; Sc: Scorodite; Sch: Schultenite; Dus: Dussertite.

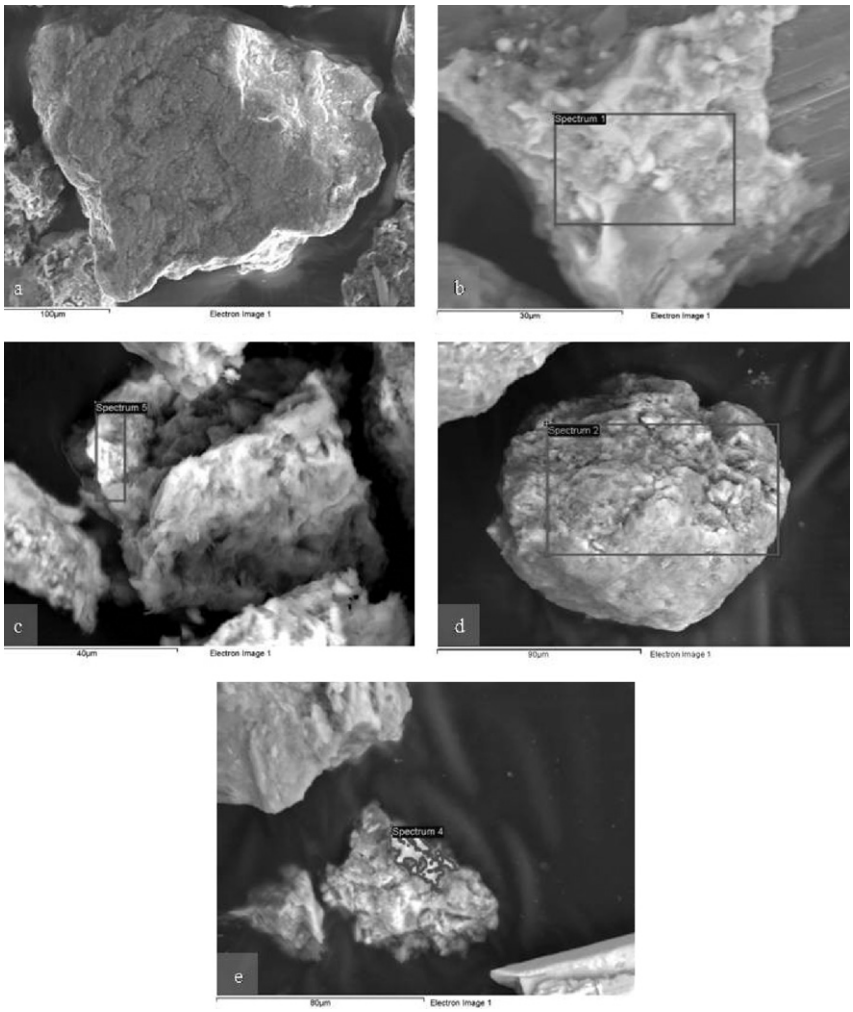

Fig. 4. Backscattering electronic image of samples with highest arsenic contents. (a) Co-107; (b) Co-142-1; (c) Co-142-2; (d) Co-150-1; (e) Co-150-2. Lighter areas correspond to the presence of element with high atomic number.

using a scanning electron microscope JEOL 6460LV, operating at 30 kV and equipped with backscattered electron detector (BEI). With this detector, the clearer areas correspond to those with a higher concentration of heavy elements. Subsequently, energy dispersive X-ray (EDX) microanalysis was performed.

3. Results and discussion

Table 2 shows the data for the sequential extraction, as well as, total and labile fraction of arsenic in soils. The results indicate that arsenic is distributed in the residual fraction from sequential extraction and the fraction bound to iron and manganese oxides. The percentages of amorphous iron are shown in Table 3. We can observe that the values of amorphous iron respect to total iron are very low. These results indicate the low mobility of arsenic in the soils studied.

The data obtained by XRD (Fig. 3) shows the presence of goethite and lepidocrocite as iron mineral phases. The values obtained by EDX (Table 4) confirm the results of XRD. According to Filippi et al. [10], Appelo et al. [32] and Manaka [33], crystalline and amorphous forms of iron affect the degree of adsorption of arsenic. Fuller et al. [34]) found that the adsorption of arsenic by more amorphous forms (e.g. ferrihydrite) is higher than the crystalline forms (e.g. goethite and hematite). However, Filippi et al. [10] found that these crystalline forms were stable when the Fe/As ratio were higher. Our results are in agreement with these authors, where mineral phases (goethite and lepidocrocite) indicate a very high Fe/As ratio (Table 4).

The X-ray microfluorescence mapping shows strong relationship between Fe and As (Fig. 2). The punctual data of arsenic percentages obtained with this technique (Table 5) allowed to chose the samples with highest arsenic contents in the fraction of 200–50 μm The next step was the study by SEM–EDX of the selected samples to verify the presence of secondary minerals of arsenic found by XRD. These secondary minerals are arsenates of iron (scorodites and angelellite), lead arsenate (schultenite) and iron and barium arsenate (dussertite) (Fig. 3).

Table 4 shows the values of chemical analysis by EDX. To select an area to perform the microprobe analysis, images from different regions of the soil samples using the backscattered electron detector were obtained (Fig. 4). The lighter areas indicate higher concentration of elements with higher atomic numbers. The arsenic content ranging from 0.65% to 21.33%. These values, with those contained in lead, iron and barium, confirming the results obtained by XRD. The lowest As percentages (0.65%), with high Fe and O contents suggest that arsenic is combined with iron oxy(hidr)oxides phases [29]. The highest As percentages (18.9% and 21.33%) seem to favour the hypothesis of presence of iron arsenates (scorodites and angelellite) [30]. On the other hand, the As intermediate contents (4.50% and 3.17%) could be related to iron and lead arsenates

Only in the Co-142-1 sample the presence of sulfur is observed (Table 4) probably due to the presence of arsenopyrite, although the

diffractograms does not show the characteristic diffraction peaks (Fig. 3). This may be because the percentage is very low. The presence of these sulphides is related to reducing redox conditions [35]. The oxidation of arsenopyrite originates scorodites [36].

Filippi et al. [10], Drahota and Filippi [13], Mahoney et al. [37] and Mains et al. [38] found that under acidic conditions, as is the case of sample studied (Table 6), scodorite is the most common arsenic secondary mineral, both in naturally contaminated soils, as well as, those contaminated by industrial and mining activities.

Scorodite solubility has been studied by many authors [39–41]. Langmuir et al. [40] studied the relationship between the scorodite solubility and soil pH, finding the lowest levels of arsenic at pH 2.5. Harvey et al. [39] found that this concentration of arsenic in soil decreased if there were many iron oxyhydroxides (ferrihydrite and goethite), being lower in the case of ferrihydrite. However, Bluteau and Demopolus [41] found that the scorodite solubility was very low in a pH range from 5 to 9, which is precisely the pH of the studied soils (Table 6).

Angelellite was found in subsurface samples (Co-138-2 and Co-142-2). This mineral has a relatively low solubility in a wide range of soil pH conditions [42,43].

Finally, we have also found diffraction peaks corresponding to schultenite and dussertite (Fig. 3). Both minerals are found in relatively small quantities and only in some samples (Co-142-1, Co-142-2, Co-150-1 and Co-150-2) (Fig. 4 and Table 4). The schultenite has low solubility in soils with pH less than 5 and high concentrations of Pb (II) and As (V) [44].

4. Conclusions

The result of the sequential extraction shows that arsenic is distributed between the iron oxides and residual fraction. This implies that arsenic is not very mobile and therefore it can be considered that a risk on this contaminated must not be assumed.

The study of heavy minerals, separated from the 200–20 μm fraction, by X-ray microfluorescence indicates the relationship between arsenic and iron oxides. In this respect, the analysis by XRD shows the existence of goethite and lepidocrocite as the main iron oxides and the presence of secondary minerals of arsenic (scorodites, angelellite, schultenite and dussertie). These minerals have a low solubility, responsible for the low availability of arsenic in the study area. This confirms the findings obtained from the sequential extraction results.

The use of SEM with backscattered electron detector allowed to define more clearly areas with higher concentrations of elements with high atomic number. The EDX microanalysis of these areas confirmed the association between iron and arsenic and revealed the existence of lead and barium in some cases. The results obtained with this technique confirmed the existence of minerals observed by XRD.

The proposed methodology, using together microfluorescence and SEM–BEI with EDX has shown great efficiency in the identification of mineral forms of arsenic in soils.

The proposed combination of methods can be used to identify mineral phases of arsenic in any sample, including those with low content of arsenic bound to the residual fraction. This methodology also allows to determine the arsenic bound to different soil fractions, as well as, easy mobilizable arsenic. Therefore, these techniques can be used to establish the level of arsenic contamination risk in soils.

Acknowledgments

We thank José María Sanabria Monge of the electronic microscopy service of CITIUS (Center for Research, Technology and Innovation at the University of Seville) for his help in the detection and interpretation of results obtained in the SEM–BEI–EDX soil analysis. We also thank Santiago Medina Carrasco, Alberto Ortega Galvan and Francisco Rodriguez Padial of X-ray laboratory of CITIUS for XRF and XRD analysis.

References

[1] B.K. Mandal, K.T. Suzuki, Talanta 58 (2002) 201–235.
[2] M. Herbel, S. Fendorf, Chem. Geol. 228 (2006) 16–32.
[3] J.E. Fergusson, The Heavy Elements: Chemistry, Environmental Impacts and Health Effects, Pergamon Press, Oxford, 1990.
[4] J.O. Nriagu, Arsenic in the Environment. Part I: Cycling and Characterization, John Wiley & Sons, New York, 1994.
[5] G.S. Camm, H.J. Glass, D.W. Bryce, A.R. Butcher, J. Geochem. Explor. 82 (2004) 1–15.
[6] B. Cancès, F. Juillot, G. Morin, V. Laperche, D. Polya, D.J. Vaughan, J. Hazemann, O. Proux, G.E. Brown Jr., G. Calas, Sci. Total Environ. 397 (2008) 178–189.
[7] K. Fukushi, M. Sasaki, T. Sato, N. Yanase, H. Amano, H. Ikeda, Appl. Geochem. 18 (2003) 1267–1278.
[8] E. Ferreira da Silva, C. Zhang, L. Serrano Pinto, C. Patinha, P. Reis, Appl. Geochem. 19 (2004) 887–898.
[9] A.K. Ghosh, D. Sarkar, P. Bhattacharyya, U.K. Maurya, D.C. Nayak, Geoderma 136 (2006) 300–309.
[10] B.M. Filippi, V. Doušová, V. Machovič, Geoderma 139 (2007) 154–170.
[11] D. Strawn, H. Doner, M. Zavarin, S. McHugo, Geoderma 108 (2002) 237–257.
[12] H. Pfeifer, A. Gueye-Girardet, D. Reymond, C. Schlegel, E. Temgoua, D.L. Hesterberg, J.W. Chou, Geoderma 122 (2004) 205–234.
[13] P. Drahota, M. Filippi, Environ. Int. 35 (2009) 1243–1255.
[14] C. Reimann, J. Matschullat, M. Birke, R. Salminen, Appl. Geochem. 24 (2009) 1147–1167.
[15] P. Tume, J. Bech, L. Longan, L. Tume, F. Reverter, B. Sepulveda, Ecol. Eng. 27 (2006) 145–152.
[16] E. Galán, J.C. Fernández-Caliani, I. González, P. Aparicio, A. Romero, J. Geochem. Explor. 98 (2008) 89–106.
[17] M. Sierra, F.J. Martínez, J. Aguilar, Geoderma 139 (2007) 209–219.
[18] K. Sultan, N.A. Shazili, J. Geochem. Explor. 103 (2009) 57–68.
[19] A. Tessier, P.G.C. Campbell, M. Bisson, Anal. Chem. 51 (1979) 844–851.
[20] W.W. Wenzel, N. Kirchbaumer, T. Prohaska, G. Stingeder, E. Lombi, D.C. Adriano, Anal. Chim. Acta 436 (2001) 309–323.
[21] S. Garcia-Manyes, G. Jiménez, A. Padró, R. Rubio, G. Rauret, Talanta 58 (2002) 97–109.
[22] A. Courtin-Nomade, C. Grosbois, H. Bril, C. Roussel, Appl. Geochem. 20 (2005) 383–396.
[23] A. Manceau, M. Lanson, N. Geoffroy, Geochim. Cosmochim. Acta 71 (2007) 95–128.
[24] S.K. Kennedy, W. Walker, B. Forslund, Environ. Forensic 3 (2002) 131–143.
[25] A.N. Halliday, J.G. Mitchell, Earth Planet. Sci. Lett. 68 (1984) 229–239.
[26] FAO-ISRIC-ISSS, World Reference Base for soil resources, 84 World Soil Resources Report. FAO. Rome, 1998.
[27] F. Guitián, T. Carballas. Técnicas de análisis de suelos. Ed. Pico Sacro. Santiago de Compostela 1976.
[28] J. Bech, C. Poschenrieder, M. Llugany, J. Barcelò, P. Tume, J. Tobías, J.L. Barranzuela, E.R. Vázquez, Sci. Total Environ. 203 (1997) 83–91.
[29] I. de Gegori, E. Fuentes, D. Olivares, H. Pinochet, J. Environ. Monit. 6 (2004) 38–47.
[30] V. Matera, I. Le Hécho, A. Laboudigue, P. Thomas, S. Tellier, M. Astruc, Environ. Pollut. 126 (2003) 51–64.
[31] P. Bhattacharyya, S. Tripathy, Kanjoo Kim, Seok-Huw Kim, Ecotoxicol. Environ. Saf. 71 (2008) 149–156.
[32] C.A.J. Appelo, D.W. Van, C. Tournassat, L. Charlet, Environ. Sci. Technol. 36 (2002) 3096–3103.
[33] M. Manaka, Geoderma 136 (2006) 75–86.
[34] C.C. Fuller, J.A. Davis, G.A. Waychunas, Geochim. Cosmochim. Acta 57 (1993) 2271–2282.
[35] M.C.F. Magalhaes, Pure Appl. Chem. 74 (2002) 1843–1850.
[36] M. Filippi, V. Goliáš, Z. Pertold, Environ. Geol. 45 (2004) 716–730.
[37] J. Mahoney, D. Langmuir, N. Gosselin, J. Rowson, Appl. Geochem. 20 (2005) 947–959.
[38] D. Mains, D. Craw, Geol.F N.Z.J., Geophysics 48 (2005) 641–647.
[39] M.C. Harvey, M.E. Schreiber, J.D. Rimstidt, M.M. Griffith, Environ. Sci. Technol. 40 (2006) 6709–6714.
[40] D. Langmuir, J. Mahoney, J. Rowson, Geochim. Cosmochim. Acta 70 (2006) 2942–2956.
[41] M Bluteau, G.P. Demopoulos, Hydrometallurgy 87 (2007) 63–177.
[42] E. Krause, V.A. Ettel, Am. Mineral. 73 (1988) 850–854.
[43] V. Matera, I. Le Hécho, in: H.M. Selim, D.L. Sparks (Eds.), Heavy Metals Release in Soils, CRC Press, Boca Raton Florida, 2001, pp. 207–231.
[44] M.C.F. Magalhaes, M.C.M. Silva, Monatsh. Chem. 134 (2003) 735–743.